

EFFECT OF DEPOSITION TIME ON ZnO/ZnS CORESHELL NANOSTRUCTURES ON SILICON SUBSTRATE

T. Y. YU^a, K. Y. WANG^b, Y. T. CHEN^b, M. L. SHEU^b, H. CHEN^{b*}

^a*Department of Information Management, National Chi Nan University, Taiwan, ROC*

^b*Department of Applied Material and Optoelectronic Engineering, National Chi Nan University, Taiwan, ROC*

In this study, core/shell structured ZnO/ZnS was grown by hydrothermal methods on silicon substrates. To study the effect of deposition time, multiple material analyses were performed on the nanostructures. Results indicate that ZnS/ZnO nanostructures with appropriate ZnS deposition time had the strongest ZnS crystalline structures. Moreover, the defect concentration would increase with the increase of the deposition time. The ZnS/ZnO nanostructures show promising for future development of sulfur-contained ZnO-based nanodevices in the future.

(Received February 8, 2017; Accepted April 3, 2017)

Keyword: ZnO/ZnS, Hydrothermal, Deposition time, Sulfur, Defect

1. Introduction

ZnO and ZnS, two direct band gap II-VI compounds, have been intensively explored as optoelectronic materials for manufacturing electronic and photonic devices since the end of the 20th century. Zinc oxide nanostructures such as nanorod, nanotube, and nanowire[1] have attracted great attention due to their promising merits of higher carrier mobility[2], ease of crystallization[3], facile production[4] and inexpensive [5][6]. Zinc oxide is an n-type semiconductor which has wide and direct band gap(3.37ev) with large exciton binding energy (60mev) has many promising applications[15], such as transducers[16], gas sensors[17], and optical devices[18]. On the other hand, ZnS is also an advantageous material, owing to its wide and direct band gap(3.67ev)[19]. Because of the existing of polar surface[20], well transport properties[21], and high electric mobility[22], ZnS nanostructures have attracted many attention in fabricating nanodevices, such as field emitters, light sensor, biological applications, optical devices electroluminescence, light-emitting diodes(LED), and electroluminescence[23]. ZnS nanotube structure has been attracted peculiar attention due to its superior properties, such as lower density, higher specific surface area, and better permeability compared with other nanostructure with high improvement for surface-related applications [24].

Combination of ZnO and ZnS structures might obtain the merits of the two materials. Recently, ZnS/ZnO nanostructures emerged as components of novel solar cells and photodetectors. Furthermore, core/shell structured ZnO/ZnS have been proposed to improve physical and chemical properties of ZnO nanostructures. Therefore, intensive studies have been made to control fabrication of ZnO/ZnS core/shell and obtain different morphologies [25]. In this study, we investigate the effect of deposition time on material properties of ZnO/ZnS Coreshell nanostructures. Multiple material characterization including FESEM, XRD, PL XPS, and surface contact angle measurements were used to study the influence of deposition time on the ZnO/ZnS

*Corresponding author: hchen@ncnu.edu.tw

Core-shell nanostructures. Results indicate that ZnS/ZnO nanostructures with appropriate ZnS deposition time had the strongest ZnS crystalline structures. Moreover, the defect concentration would increase with the increase of the deposition time.

2. Experimental

In the beginning, silicon wafers were cut into $2 \times 2 \text{ cm}^2$ silicon substrates, and then carry on the cleaning procedure. There are six steps of cleaning procedure. After the substrates were cleansed in the mixture of H_2SO_4 and H_2O_2 for 10 minutes, they were immersed in the HF solution to remove the native oxide. To fabricate ZnO seed layers on the silicon substrate, 0.66 g of $\text{Zn}(\text{CH}_3\text{COO})_2$ was dispersed in 60 ml of ethanol and then the solution was added with few drops of monoethanolamine (MEA). Then, the solution was stirred at 60°C for 30 minutes and placed at room temperature for 24 hours. After 24 hours, the solution became transparent. To grow seed layer on the cleansed substrate, a few drops of the resultant solution was dripped on the substrate. Then, the substrate was spin-coating method for 30 seconds, then heated at 130°C for 5 minutes. To grow ZnO nanorods, 0.9468 g of $\text{Zn}(\text{NO}_3)_2$ and 0.9812 g of hexamethylenetetramine (HMTA) was dispersed in the 100 ml distilled water. The substrate was immersed in the growth solution and the ZnO nanorods were grown by hydrothermal method at 80°C for 1 hour. In order to cover the surface of ZnO nanorods with ZnS, ZnO nanorods was immersed in the solution which contained 2.4018 g of $\text{Na}_2\text{S} \cdot 9\text{H}_2\text{O}$ for 5, 10, 20, and 30 minutes to form core/shell structured ZnO/ZnS.

3. Results and discussions

To characterize ZnS layer coated on ZnO nanorods growth for various time, FESEM images were taken to view the surface morphology of the ZnS/ZnO structures. For the ZnO nanorods without ZnS layer, smoothy and clean surface on the rod side and top surface could be observed as shown in Fig.1 (a). After ZnS was deposited for 5 min to 10 min, fluffy structures emerged to appear on the side surface as shown in Fig.1 (b) and (c). As the ZnS deposition time lengthened to 20 min to 30 min, the fluffy surface could still be observed as shown in Fig.1 (d) and (e), but the surface was not as uneven as the surface of the ZnS deposited for 5 and 10 min.

To analyze the crystalline phases of the ZnS/ZnO nanocomposite, XRD was used to investigate the structures as shown in Fig.2. Obviously the ZnO crystalline phases became weaker and weaker as the ZnS deposition time increased. Since the deposited ZnS might cover ZnO NRs and transform the material properties, ZnO phases became weaker. On the other hand, ZnS (111) phases emerged after ZnS was deposited for 5 min. However, as the ZnS deposition time increased more than 10 min, the (111) ZnS phase disappeared. The result was consistent with FESEM images. The most fluffy structure occurred as ZnS deposited for 5 min.

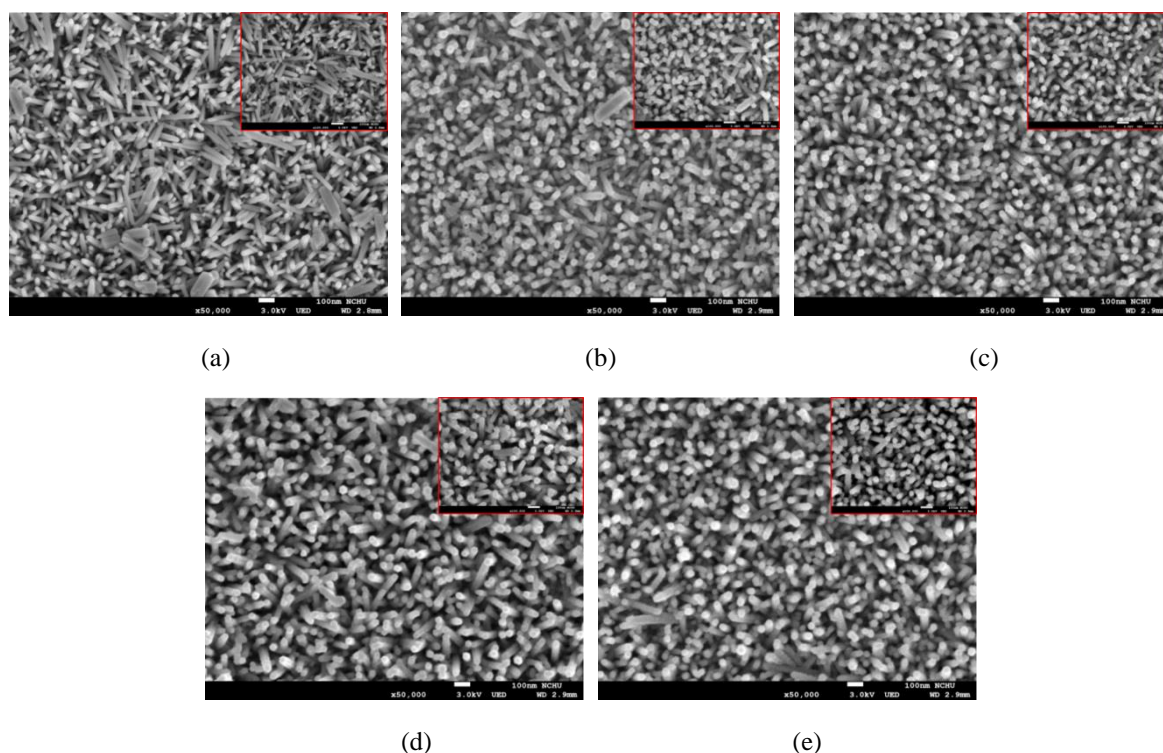


Fig.1 FESEM images of the ZnS/ZnO nanostructures with deposition time of (a) 0 min (b) 5 min (c) 10min (d) 20min (e) 30min

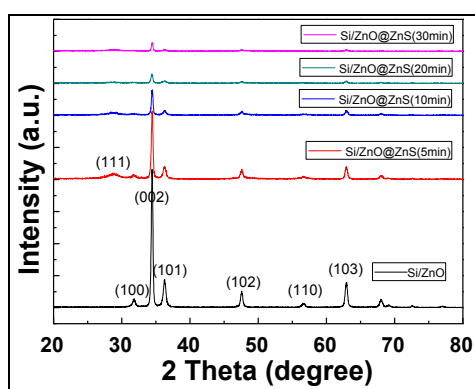


Fig.2 XRD patterns of the ZnS/ZnO structures with different ZnS deposition time.

To further analyze the material properties of the ZnS/ZnO structures, PL and XPS were used to analyze the presence of the defect and the chemical binding, respectively. PL measurements as shown in Fig.3 reveal that the defect luminescence, which was around 560 nm, increased drastically as the ZnS deposition time increased from 20 sec to 30 sec. The result indicated that plenty of defects in ZnS/ZnO might be generated during the growth time from 20 min to 30 min. To further study the detailed mechanism, the S 1s XPS was used to analyze the S binding as shown in Fig. 4. In the S 1s XPS spectrum, the sudden increase of S as shown in Fig. 4

might cause the sudden increase of the defect luminescence. In addition, the appearance of defects might damage the original ZnS structure as revealed in the XRD and FESEM images.

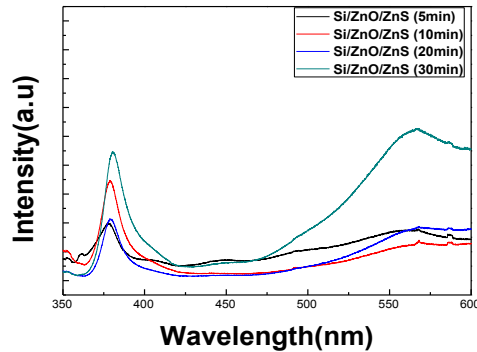


Fig.3 PL measurements of the ZnS/ZnO structures with different ZnS deposition time.

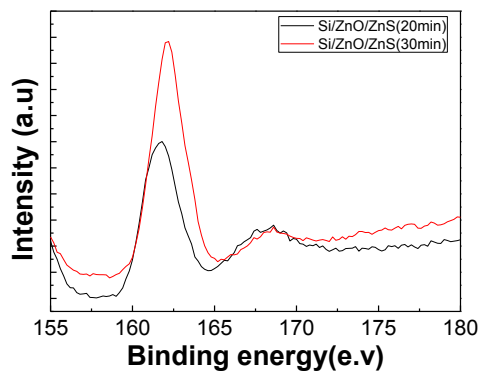


Fig.4 The S 1s XPS spectra of the ZnS/ZnO with ZnS deposition time of 20 and 30 min.

Finally, the surface contact angle measurements were performed for the ZnS/ZnO nanostructures with various deposition times. Fig. 5 (a)-(e) show the contact angle measurements for the ZnS/ZnO structures with ZnS deposition times of 0, 5, 10, 20, and 30 min, respectively. The results indicate that the longer the ZnS deposition time was, the larger surface contact angle would have, signifying that the ZnS and the defect nanostructure could enhance the hydrophobic properties. The graph of the ZnS deposition time versus the surface contact angle is shown in Fig. 5 (f).

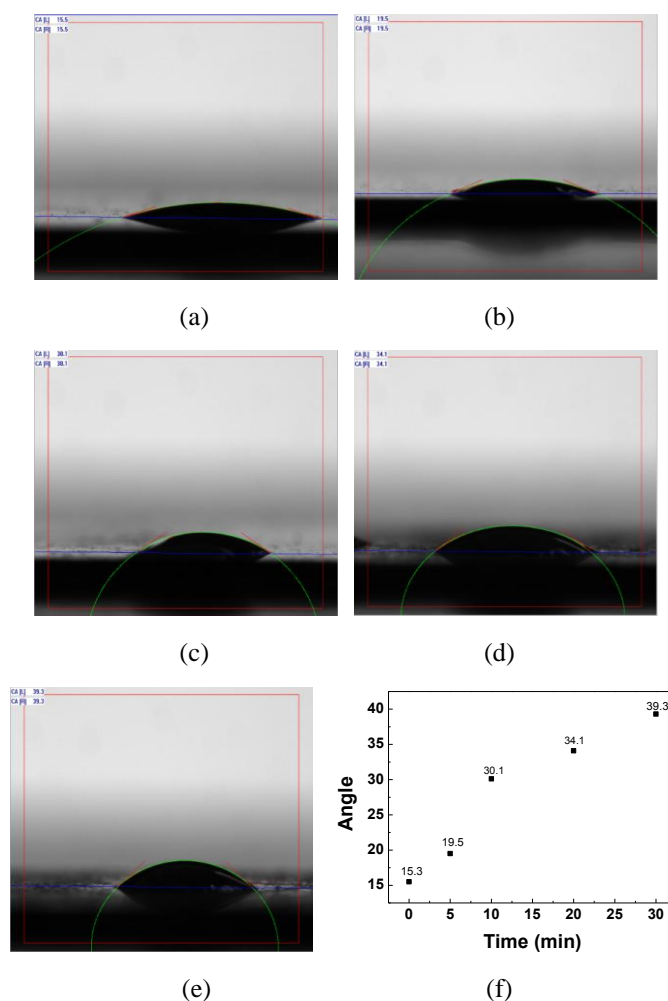


Fig. 5 Surface contact angle measurements of the ZnS/ZnO nanostructures with ZnS deposition time of (a) 0 (b) 5 (c) 10 (d) 20 (e) 30 min (f) The graph of the contact angle versus the ZnS deposition time.

4. Conclusions

In this study, ZnS/ZnO nanostructures were formed by depositing ZnS layer on the ZnO nanorods. To characterize the material properties of the ZnS/ZnO structures, multiple material analyses including FESEM, XRD, PL, XPS and surface contact angle were performed. Results indicate that ZnS/ZnO nanostructures with ZnS deposition time of 5 min had the strongest crystalline ZnS structures.

As the deposition time increased more than 20 mins, the increase of sulfur content might enhance the generation of defects and damage the ZnS crystalline structures. The ZnS/ZnO nanostructures show promising for future development of sulfur-contained ZnO-based nanodevices in the future.

References

- [1] Z. Fan, J. G. Lu, Journal of nanoscience and nanotechnology **5**, 1561 (2005).
- [2] C. Jagadish, S. J. Pearton, Jagadish, S.J. Pearton, Zinc oxide bulk, thin films

- and nanostructures: processing, properties, and applications. 2011: Elsevier.
- [3] R. Laudise, A. Ballman, *The Journal of Physical Chemistry* **64**, 688 (1960).
 - [4] N. Bao, L. Shen , T. Takata , K. Domen , A. Gupta ,K. Yanagisawa , C. A. Grimes, *The Journal of Physical Chemistry C* **111**, 17527 (2007).
 - [5] L.E. Greene, M. Law , J. Goldberger, F. Kim, J.C. Johnson, Y. Zhang, R. J. Saykally, P. Yang, *Angewandte Chemie* **115**, 3139 (2003).
 - [6] O. Lupan, L. Chow, G. Chai, B. Roldan, A. Naitabdi, A. Schulte, H. Heinrich, *Materials Science and Engineering: B* **145**, 57 (2007).
 - [7] J. J. Wu, S.C. Liu, *Advanced Materials* **14**, 215 (2002).
 - [8] G. Jimenez-Cadena, E. Comini, M. Ferroni, A. Vomiero, G. Sberveglieri, *Materials Chemistry and Physics* **124**, 694 (2010).
 - [9] S. Wei, J. Lian, H. Wu, *Materials Characterization* **61**, 1239 (2010).
 - [10] J.H. Choy, E.S. Jang, J.H. Won, J.H. Chung, D.J. Jang, and Y.W. Kim, *Advanced Materials* **15**, 1911 (2003).
 - [11] T. Minami, H. Nanto, and S. Takata, *Japanese Journal of Applied Physics* **24**, L781 (1985).
 - [12] L. Vayssieres, *Advanced Materials* **15**, 464 (2003).
 - [13] M.Y. Choi, D. Choi, M.J Jin, I. Kim, S.H. Kim, J.Y. Choi, S.Y. Lee, J.M. Kim, S.W. Kim, *Advanced Materials* **21**, 2185 (2009).
 - [14] A. Wei, X. W. Sun, C.X. Xu, Z.L. Dong, M.B. Yu, and W. Huang, *Applied Physics Letters* **88**, 213102 (2006).
 - [15] C. Soci, A. Zhang , B. Xiang , S. A. Dayeh , D. P. R. Aplin , J. Park , X. Y. Bao, Y. H. Lo , D. Wang, *Nano letters* **7**, 1003 (2007).
 - [16] M.H. Asif, S. M. Usman Alia, O. Nura, M. Willandera, C. Brännmarkb, P. Strålforsb, U.H. Englundb, F. Elinderb, B. Danielssonc, *Biosensors and Bioelectronics* **25**, 2205 (2010).
 - [17] J. Wang, X.W. Sun, Y. Yang, H. Huang, Y.C. Lee, O.K. Tan, L. Vayssieres, *Nanotechnology* **17**, 4995 (2006).
 - [18] K. Takanezawa, K. Hirota, Q.S. Wei, K. Tajima, and K. Hashimoto, *The Journal of Physical Chemistry C* **111**, 7218 (2007).
 - [19] T. B. Nasr, N. Kamouna, M. Kanzarib, R. Bennaceura, *Thin Solid Films* **500**, 4 (2006).
 - [20] D. Moore, C. Ronning, C. Ma, Z.L. Wang, *Chemical Physics Letters* **385**, 8 (2004).
 - [21] H. Yang, P.H. Holloway, B.B. Ratna, *Journal of Applied Physics* **93**, 586 (2003).
 - [22] S. Yano, R. Schroeder, H. Sakai, and B. Ullrich, *Applied physics letters* **82**, 2026 (2003).
 - [23] X. Fang, L. Wu, L. Hu, *Advanced Materials* **23**, 585 (2011).
 - [24] C.A. Amarnath, S.S. Nanda , G.C. Papaefthymiou , D.K. Yi, U.Paik, *Critical Reviews in Solid State and Materials Sciences* **38**, 1 (2013).
 - [25] T. Ghrib, M. A. Al-Messiere, A. L. Al-Otaibi, *Journal of Nanomaterials* **2014**, 1 (2014).